



# InAs quantum dots in a $\text{GaAs}_{1-x}\text{Sb}_x$ matrix for intermediate band solar cell



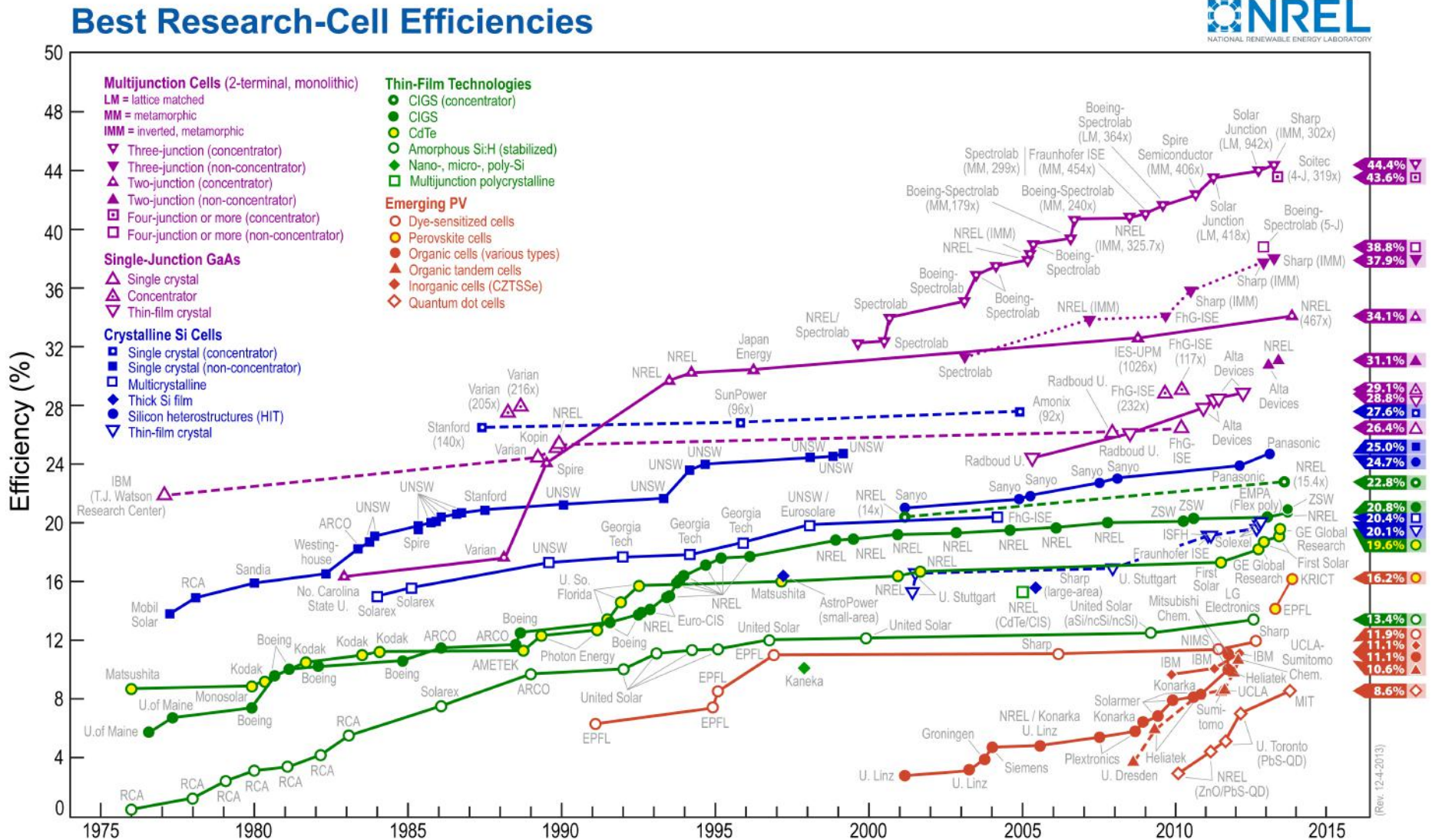
- Comparison of different solar cells.....
- Intermediate band solar cell
- Experiment data and analysis
- Conclusions and future work

Yang Cheng<sup>1</sup>, Mukul Debnath<sup>1</sup>, Vincent R. Whiteside<sup>1</sup>, Tetsuya Mishima<sup>1</sup>, Michael B. Santos<sup>1</sup>, Ian R. Sellers<sup>1</sup>, Lucas Phinney<sup>2</sup>, Khalid Hossain<sup>2</sup>

- <sup>1</sup> University of Oklahoma
- <sup>2</sup> Amethyst Research Inc.

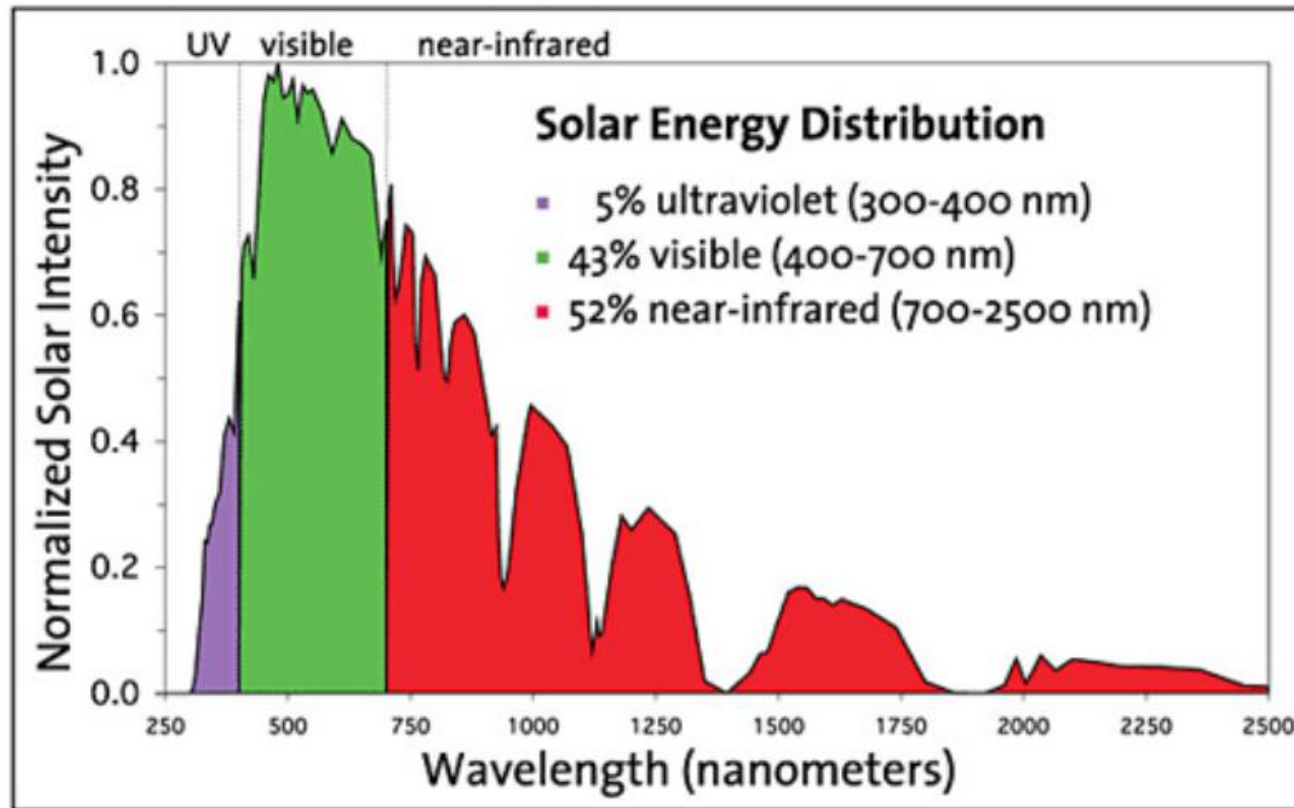


# Best Research-Cell Efficiencies





# Solar Energy Distribution



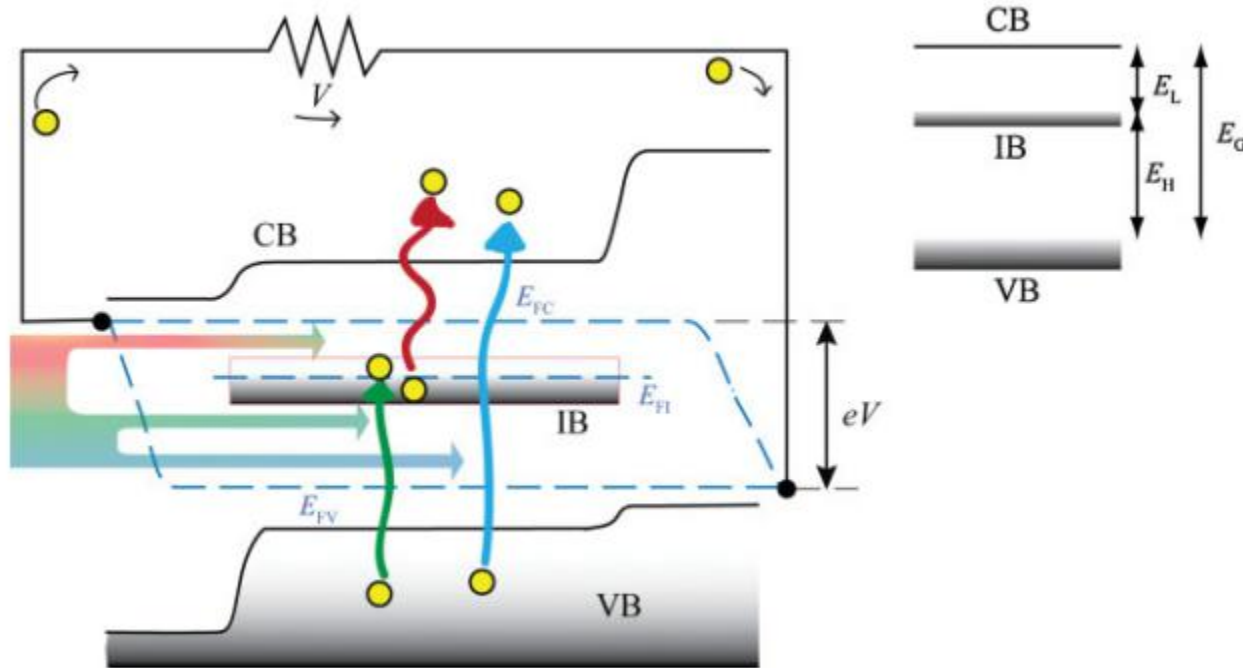
Solar energy distribution graph illustrating that infrared radiation makes up a large portion of the solar spectrum.

Graph courtesy of Berkeley Lab Heat Island Group



# Intermediate Band Solar Cells

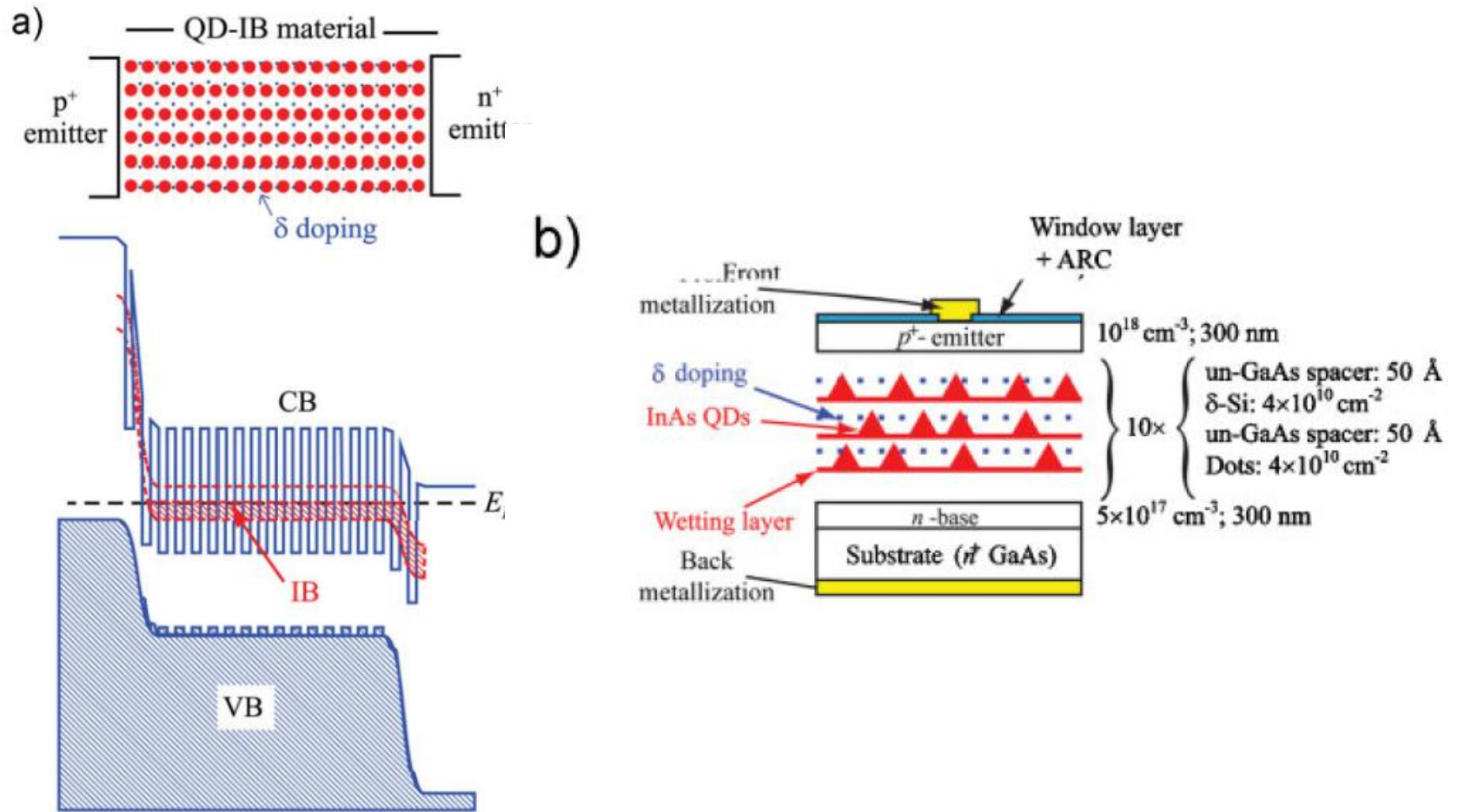
Increase the efficiency of low-cost solar cells as long as have the potential of operating with very high efficiency.



*Luque, Antonio, and Antonio Martí. Advanced Materials 22.2 (2010): 160-174.*



# Quantum Dot Intermediate band solar cell



Luque, Antonio, and Antonio Martí. *Advanced Materials* 22.2 (2010): 160-174.



# Motivation



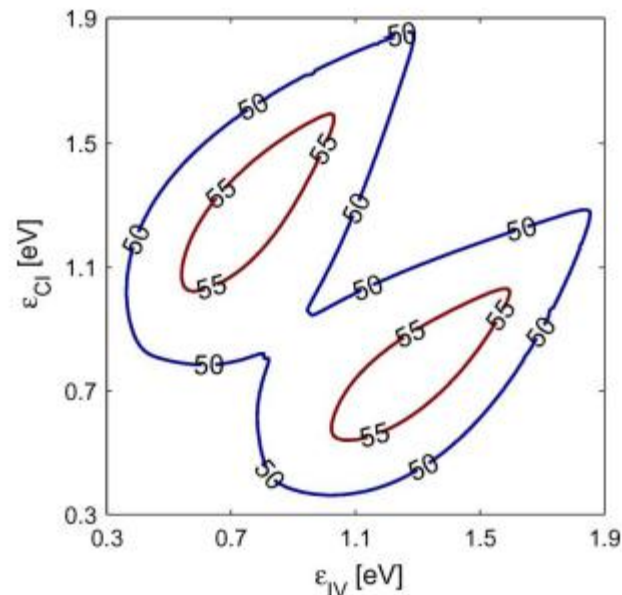
## Nanostructured Absorbers for Multiple Transition Solar Cells

Michael Y. Levy and Christiana Honsberg, *Senior Member, IEEE*

**Abstract**—This paper identifies absorbers for multiple transition solar cells that are implemented with nanostructured heterojunctions [e.g., quantum well solar cells with quasi-Fermi-level variations and quantum dot (QD) intermediate-band solar cells]. In the radiative limit, the solar cells implemented with these absorbers are capable of achieving a conversion efficiency  $\geq 50\%$  with a geometric solar concentration of at least  $1000\times$ . The technical approach enumerates a set of quantitative design rules and applies the rules to the technologically important III–V semiconductors and their ternary alloys. A novel design rule mandates a negligible valence band discontinuity between the barrier material and confined materials. Another key design rule stipulates that the substrate have a lattice constant in between that of the barrier material and that of the quantum-confined material, which permits strain compensation. Strain compensation, in turn, allows a large number of QD layers to be incorporated into the solar cell because each layer is free of defects. Four candidate materials systems (confined/barrier/substrate) are identified:  $\text{InP}_{0.85}\text{Sb}_{0.15}/\text{GaAs}/\text{InP}$ ,  $\text{InAs}_{0.40}\text{P}_{0.60}/\text{GaAs}/\text{InP}$ ,  $\text{InAs}/\text{GaAs}_{0.88}\text{Sb}_{0.12}/\text{InP}$ , and  $\text{InP}/\text{GaAs}_{0.70}\text{P}_{0.30}/\text{GaAs}$ . Resulting from the design features, the candidate systems may also find use in other optoelectronic applications.

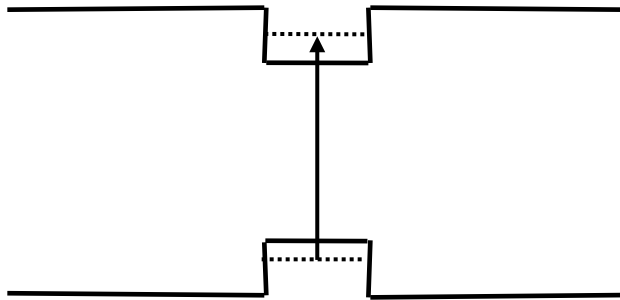
**Index Terms**—Heterojunction, intermediate band, quantum dot, quantum well, solar cell.

cell with quasi-Fermi-level variations [7] and the quantum dot (QD) intermediate-band solar cell (IBSC) [8]. It is important to note that both of these approaches may be shown to be thermodynamically consistent [9]. Until now, material systems that are

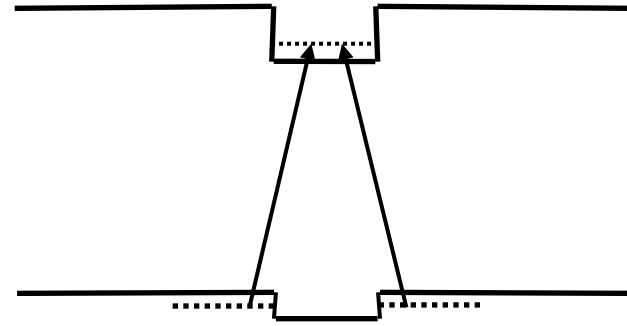




# Transition from Type I to Type II



**Type I Alignment**



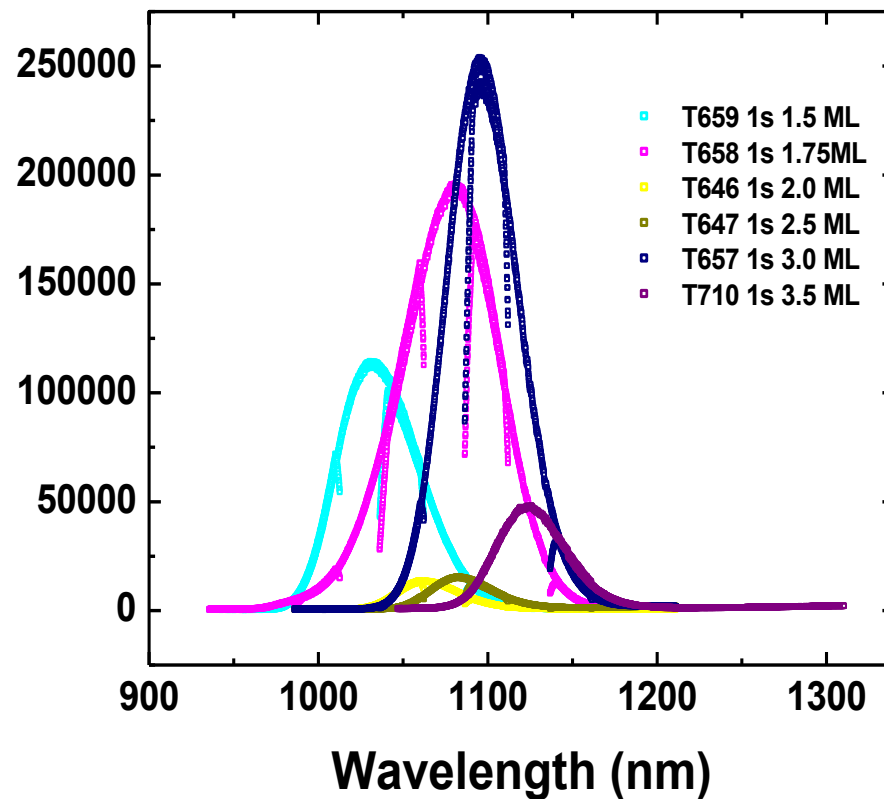
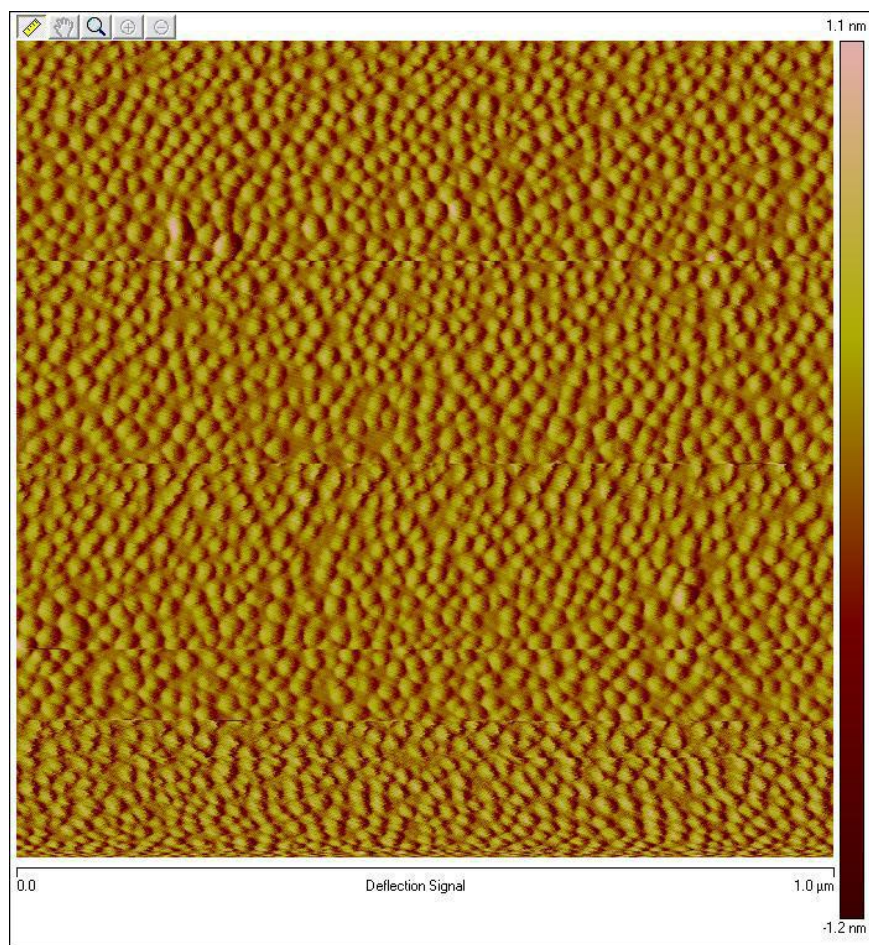
**Type II Alignment**

Type I Alignment has more oscillator strength, which gives us a high PL intensity compared with Type II Alignment.

For a Quasi-flat valence band, we should have a weaker PL due to the carrier escape for valence band.



# Experiment Data and Analysis



QDs density is nearly  $4 \times 10^{11} \text{ cm}^{-2}$





# Experiment Data and Analysis

InAs QDs	3.0 ML
GaAs <sub>1-x</sub> Sb <sub>x</sub>	50 nm
InAs QDs	3.0 ML
GaAs <sub>1-x</sub> Sb <sub>x</sub>	10 nm
GaAs Buffer	250 nm
GaAs Substrate	

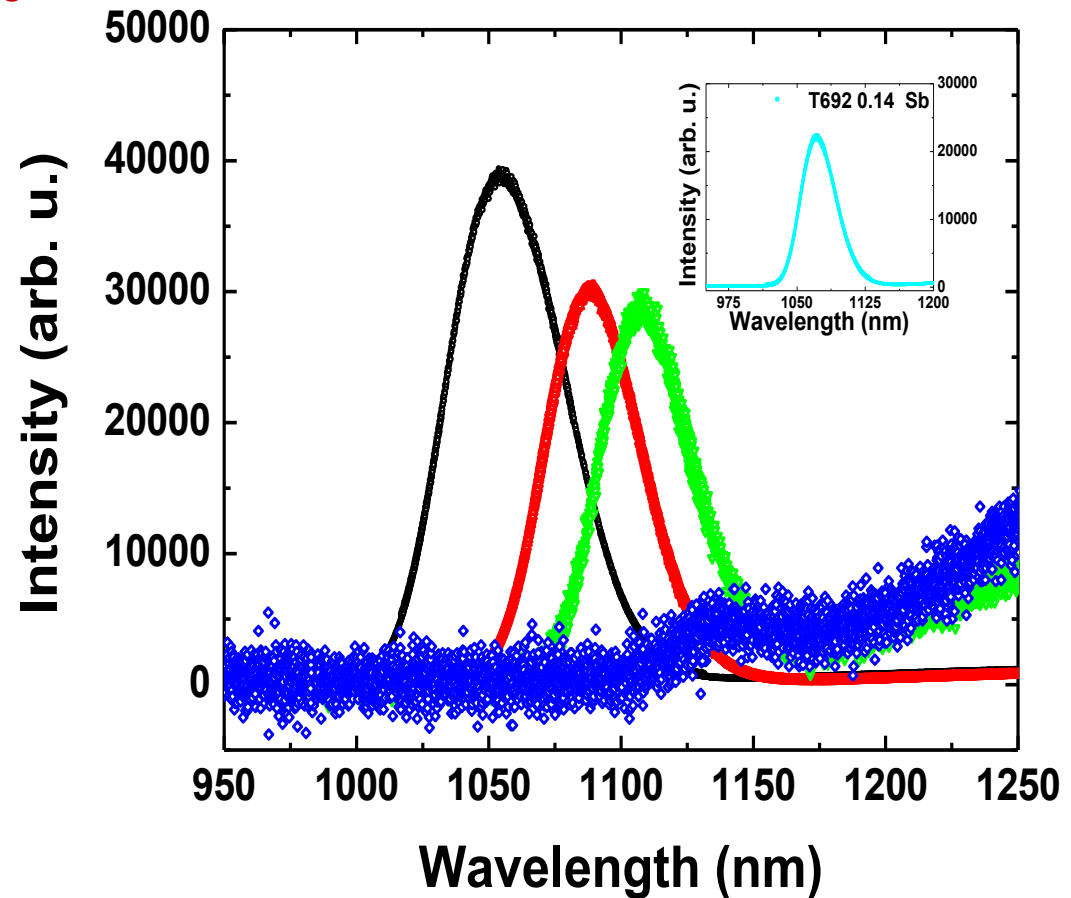
} Barrier  
Composition  
varies

- T693 0.10 Sb
- ▲ T691 0.12 Sb
- ▼ T706 0.16 Sb 50X
- ◆ T707 0.18 Sb 100X

We vary the Sb composition in the barriers from 10% to 18%

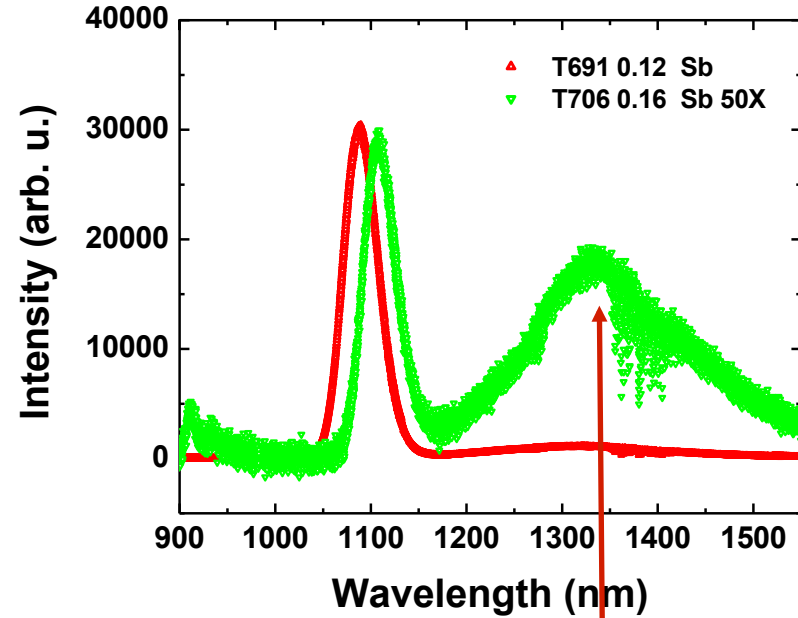
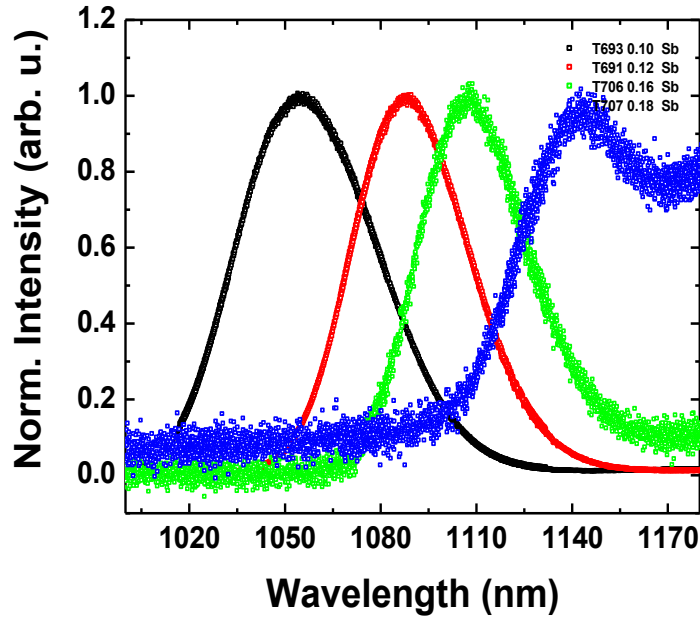
The 12% Sb gives us PL intensity two order magnitude larger than the 16%

The Sb composition increasing shows peak shift and PL intensity reduction





# 4K PL Data and Analysis



Large defects band

## Question:

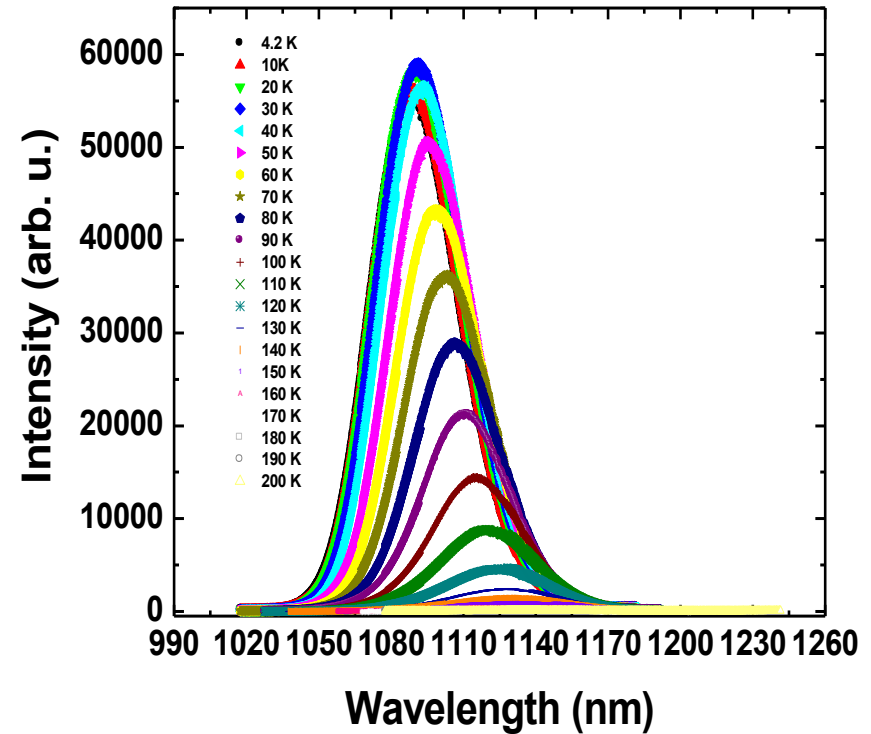
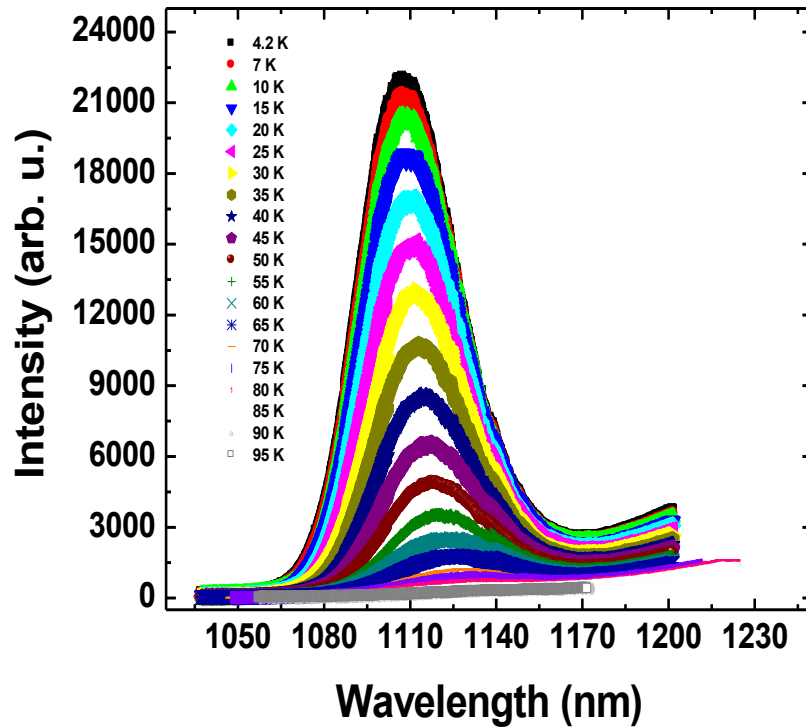
Is this reduction due to **Type I to Type II** transition or due more to **defects**?



# TD PL Data and Analysis

16% Sb

12% Sb



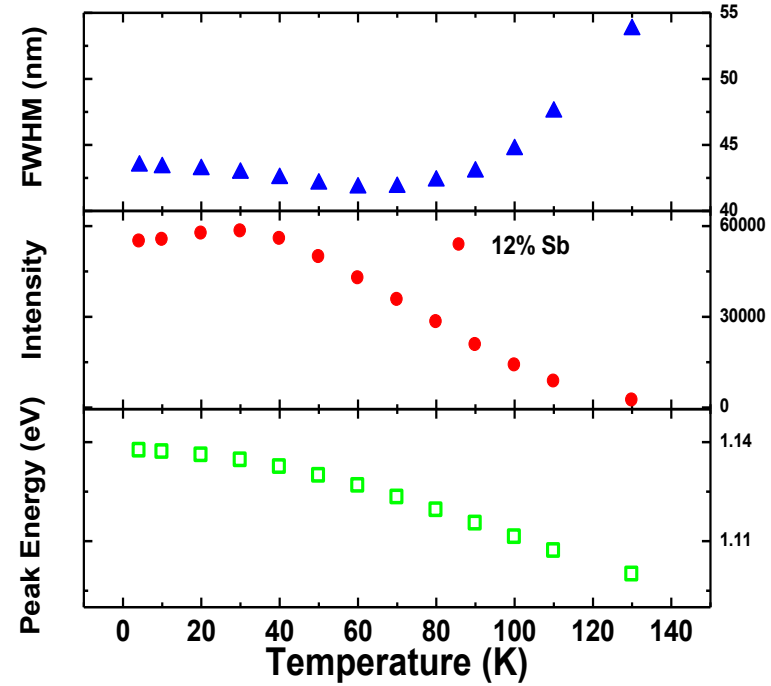
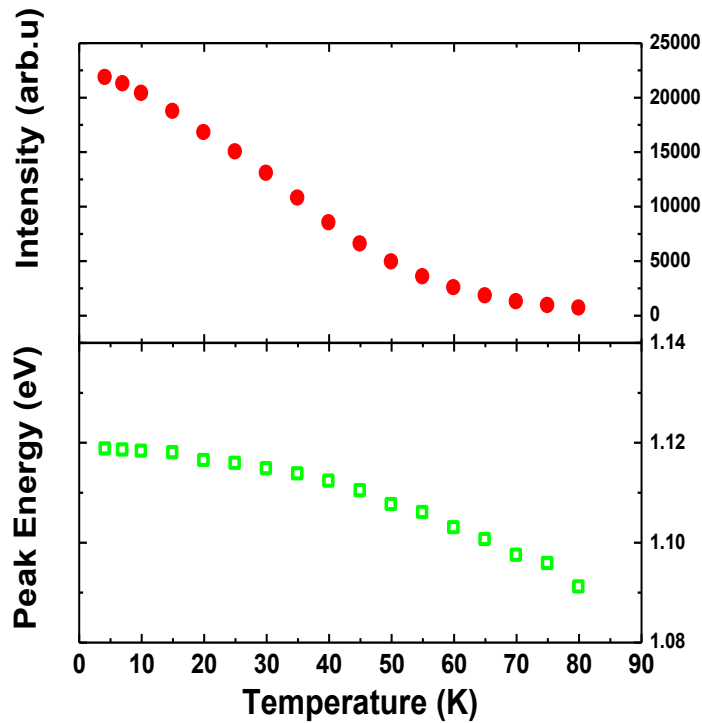
- 16% rapid reductions in PL with T and low absolute PL intensity.
- 12% classic TD PL – thermal expansion related shift.



# TD PL Data and Analysis

16% Sb

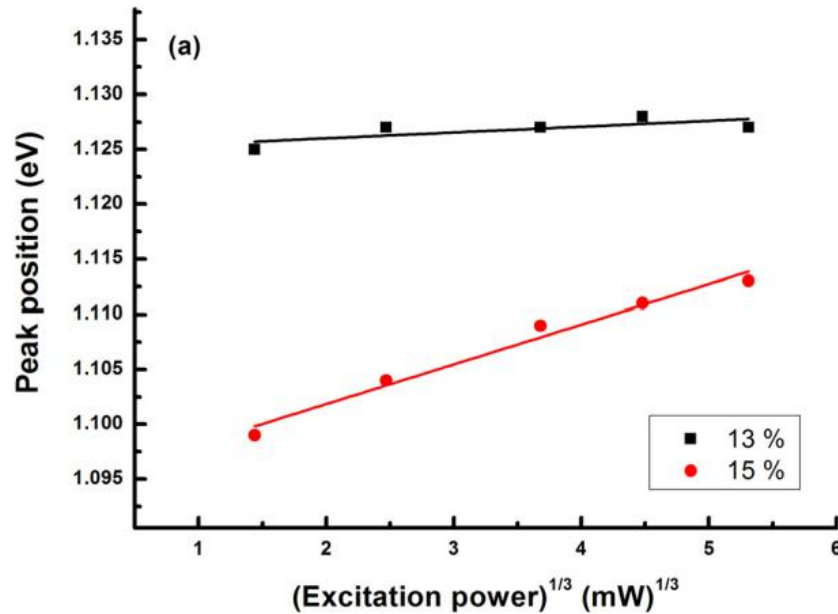
12% Sb



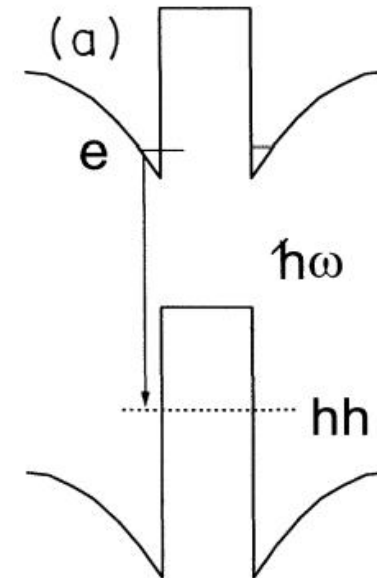
- 16% rapid reductions in PL with T and low absolute PL intensity.
- 12% classic TD PL – thermal expansion related shift.



## Transition from Type I to Type II



Ban, Keun-Yong, et al. *Journal of Applied Physics* 111.10 (2012): 104302.



At higher powers an excess of holes and electrons are created at the interface between the two semiconductors. For Type II, the spatial separation of carriers in CB and VB will induce an electric field which bends the energy level and increases the gap.

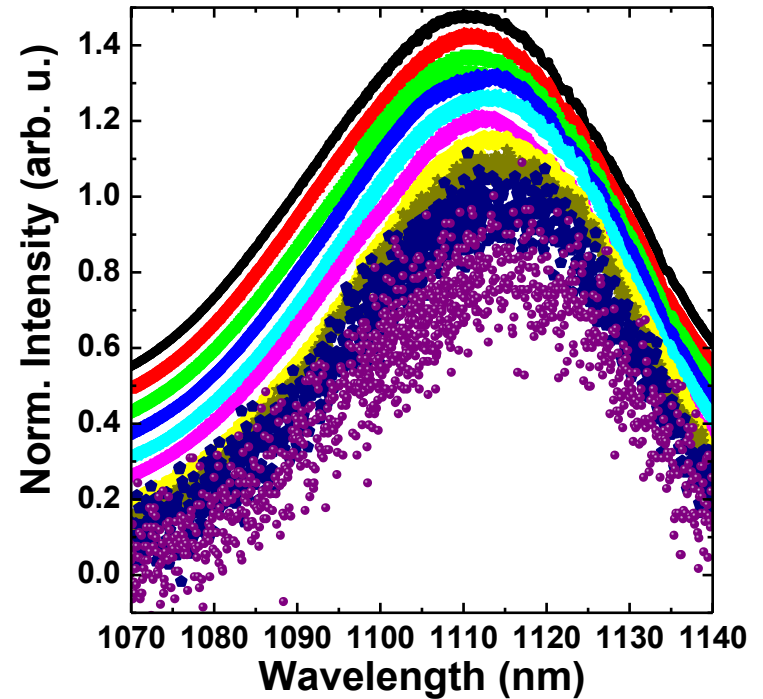
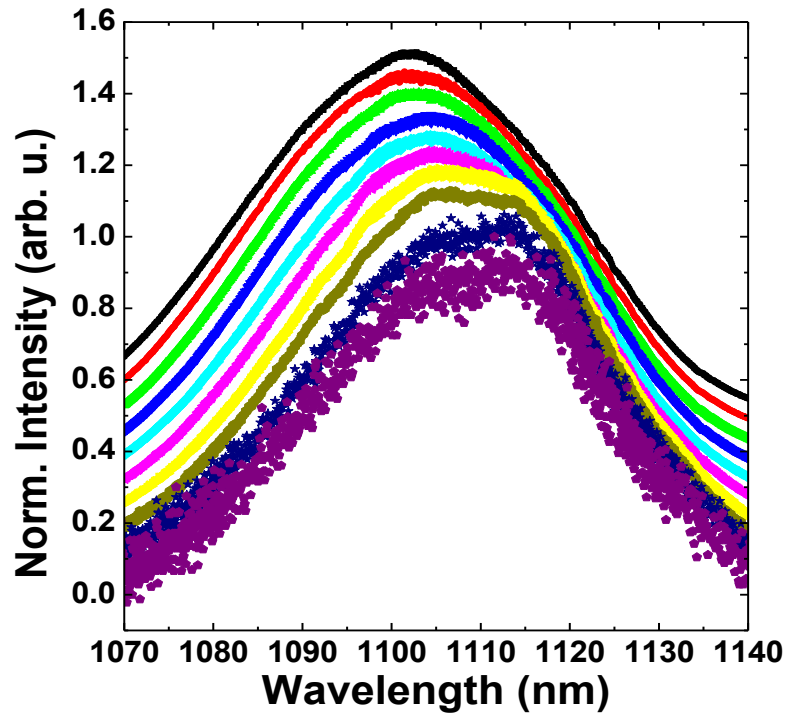
Ledentsov, N. N., et al. *Physical Review B* 52.19 (1995): 14058.



# Power Dependence Study

14% Sb

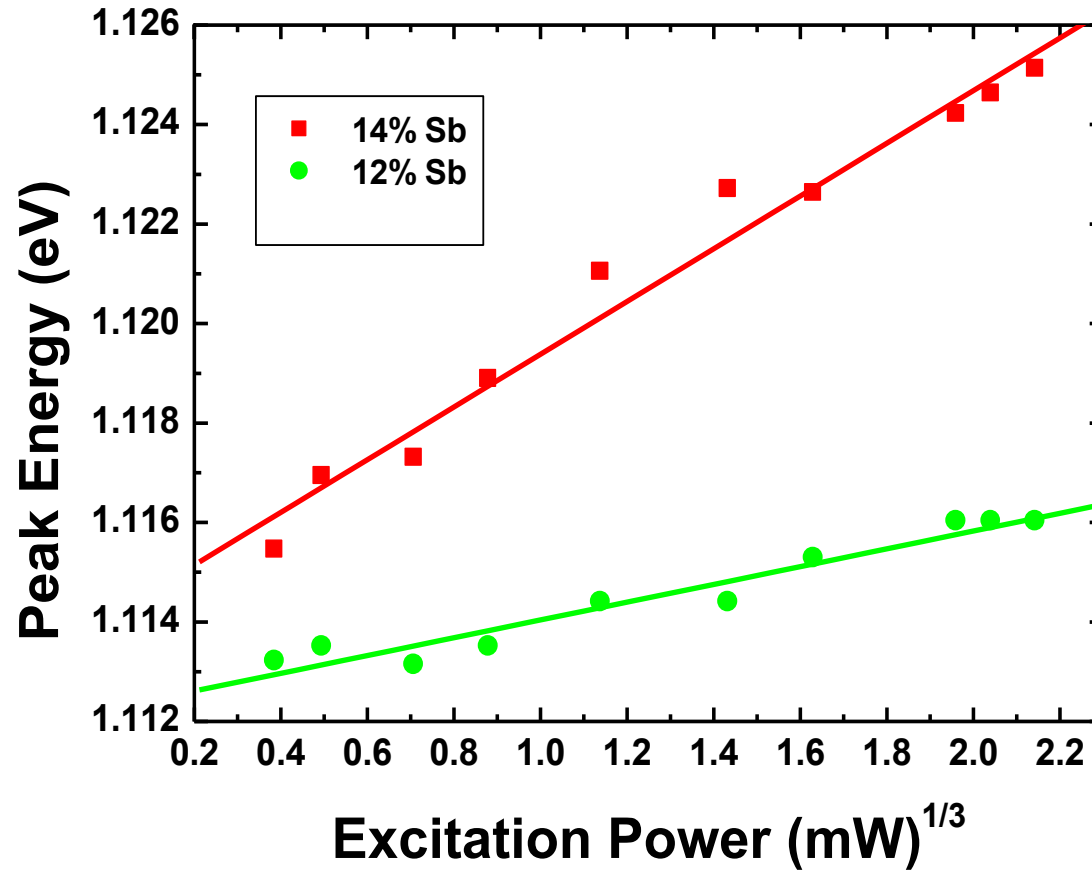
12% Sb



The energy shift of 14% is 3 times larger than the 12%



# Power Dependence Study



The energy shift of 14% is 3 times larger than the 12%



## **Conclusions:**

Optimized growth conditions for InAs QDs in “full” GaAsSb matrix.

Investigated tuning QD energy and type-I to type-II offset via Sb-composition in GaAsSb matrix: Transition evident around 14%

However, large defect band evident for increasing Sb > 12%

## **Future work:**

Investigate further defect band versus type-II in larger Sb-containing samples

Multi-layer and doped QD structures with a view to producing QD solar cells based on InAs/GaAsSb QDs system.

## **Acknowledgement:**

Research supported by the OCAST OARS program.